Microstructure and Swelling Behavior of Ion-Exchange Resin

FUMIYOSHI IKKAI and MITSUHIRO SHIBAYAMA*

Department of Polymer Science and Engineering, Kyoto Institute of Technology, Matsugasaki, Kyoto 606, Japan

SYNOPSIS

The microstructure and swelling kinetics of ion-exchange resins having sulfonic acid groups were investigated by small-angle neutron scattering (SANS) and swelling experiments as functions of the crosslinking density (CD), pH, and the salt concentration (C_{salt}). The swelling kinetics was analyzed on the basis of the Tanaka–Fillmore swelling equation for the cooperative diffusion of polymer gels. The swelling behavior was very sensitive to CD, but not to pH and C_{salt}. The SANS intensity functions, $I(q)$, were independent of CD and well described with a power law function, $I(q) \sim q^{-D}$, where q and D are the magnitude of the scattering vector and the mass-fractal dimension, respectively. D was estimated to be ~ 2, indicating that the resin consisted of a rather coarsely interconnected domains irrespective of CD at swelling equilibrium. It was found that CD is the most important parameter determining the swelling power of ion-exchange resin. However, no remarkable variations were found in the microstructure in the order of tens to hundreds of angstrom. © 1996 John Wiley & Sons, Inc.

Keywords: ion-exchange resin • swelling kinetics • small-angle neutron scattering

INTRODUCTION

Due to the great exchange capability of many kinds of ions, ion-exchange resins are widely used in various ways, such as the purification and/or dealkalization of water, collection of useful materials, sugar purification, catalyst, dehydrating agent, and so on.[1-3] Though an ion-exchange resin swollen with a large amount of water is regarded as a typical chemically crosslinked polyelectrolyte gel, the microscopic structures of the ionic resin are expected to be different from those of polyelectrolyte gels because of the difference in preparation. In the case of polyelectrolyte gels, a large number of structure investigations have been conducted to clarify the effects of charge interaction and/or Donnan membrane effect on the microscopic structures of the gels.[4-6] On the other hand, microscopic structure of ion-exchange resin has been mainly studied not on the resin itself but on its precursor, e.g., styrene-divinylbenzene copolymer made by bulk or suspension polymerization. Fernandez et al.[7] studied the state of aggregation of polystyrene-divinylbenzene networks, made by free radical polymerization, in terms of small-angle neutron scattering (SANS). They concluded that those aggregates had a size of 350–400 Å. Weissman et al.[8] discussed the inhomogeneities in crosslinked polystyrene based on SANS analysis on the conformation of the partially labeled chains in the network. Furthermore, Wojaczynska and Kolarz[9] found that the structure of copolymers of styrene and divinylbenzene (50% crosslinking degree), prepared by suspension polymerization, was influenced by the nature of solvents used for polymerization. However, none of them paid attention to the effect of the structure on the swelling behavior of the ion-exchange resin although they are closely related to the microscopic structure. An interesting work on swelling and mechanical behavior of styrene-divinylbenzene copolymers was carried out by Wieczorek et al., where they discussed the glass transition as a function of temperature or swelling.[10]

In this article, we investigated the swelling properties of cation-exchange resins as well as their precursors having several levels of crosslinking density (CD) in the circumstance of aqueous solutions with various pHs and salt concentrations, C_{salt}. Furthermore, the microstructure of the resins and precursors

was studied by SANS. The relationship between microstructure and macroscopic swelling behavior for both the ion-exchange resins and the precursors will be discussed on the basis of the CD dependence of the swelling kinetics, equilibrium swelling ratio, and the structure parameters.

EXPERIMENTAL

Samples

Ion-exchange resins and the precursors were supplied by Mitsubishi Chemical Corporation, Japan. The precursors were prepared by suspension polymerization of styrene and divinylbenzene in water. The details of precursor preparation are described elsewhere.[2,3] The ion-exchange resins were obtained by subsequent sulfonation of the precursors. The degree of sulfonation was $\sim$ 40 wt %, which was estimated by titration.[3] Thus, six kinds of precursors and cation-exchange resins each, in the form of spherical particle, were prepared having CD = 2, 4, 8, 10, 12, 16 wt % (stoichiometric).[3] Before these particles were used in the swelling and SANS measurements, the samples were freeze dried. The size of the dried particles was in the range of 200–800 μm in diameter. The pH and C_{salt} of the swelling solution were adjusted by HCl/NaOH and NaCl, respectively.

Swelling Measurement

The swelling kinetics observation was carried out as follows. As soon as a sample particle was dropped in a solution contained in a Petri dish, the time evolution of the diameter of the particle was measured with an inverted microscope coupled with a CCD (charge capacity device) camera. The fed image was sent to an electric scaler for accurate determination of the size. The swelling solvents were toluene for precursors and aqueous solutions with the different pHs or C_{salt} for ion-exchange resins.

SANS

Small-angle neutron scattering (SANS) measurements were performed on the SANS-U at the research reactor in Institute of Solid State Physics, The University of Tokyo, which is located at the Japan Atomic Energy Research Institute, Tokai, Japan. An incident wavelength of 7 Å was used. The detector was placed at 4 m from the sample, and data acquisition was conducted for 30 min for each

sample at room temperature (26 ± 1°C). Heavy water and deuterated toluene were used as solvents for ion-exchange resins and the precursors, respectively. The samples immersed in deuterated solvent were placed in quartz cells having path lengths of 1–4 mm. Radial averaging of the observed scattering intensity were taken after corrections for incoherent background, detector response, cell window scattering, and transmission. The intensity observed thereby was rescaled to the absolute intensity on the basis of the incoherent scattering from a Lupolen standard. The details of the correction are described elsewhere.[11,12]

RESULTS AND DISCUSSION

Swelling Kinetics

Figure 1 shows the time variation of the diameter of ion-exchange resin particles having several initial diameters, d_0s. These resins had the same CD of 4%. The ordinate denotes the linear swelling ratio, i.e., the ratio of the diameters at time t and before swelling, d_t/d_0, and the abscissa is the swelling time, t, from the moment of sample immersion. We can extract three interesting features of the swelling kinetics from the figure. First, the swelling is completed in a few hundred seconds, which is much faster than that of typical gels having a similar size, e.g., polyacrylamide gel.[13] Second, the smaller the initial diameter of the ion-exchange resin, the faster is the swelling kinetics. Third, the linear swelling ratio at saturation, i.e., d_∞/d_0, is independent of d_0.

Figure 2 shows CD dependencies of the swelling ratio at saturation, d_∞/d_0 for the ion-exchange resins (filled circles) and for the precursors (open circles). This indicates that (1) the final linear swelling ratio
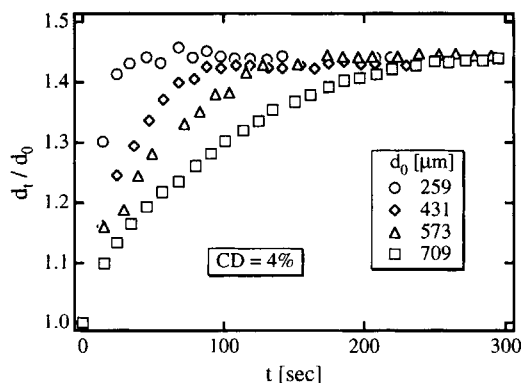

Figure 1   Time variation of the ion-exchange resins having several initial diameters, d_0s. d_t/d_0 is the ratio of the diameters after and before swelling.
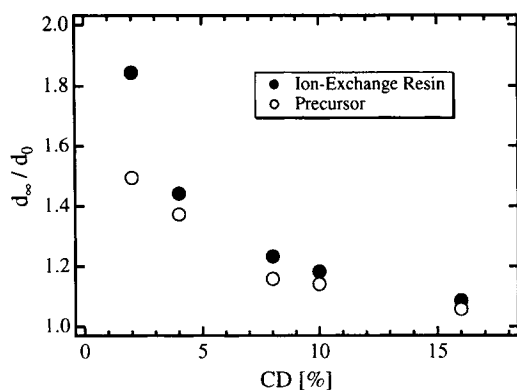
Figure 2 CD dependencies of d_α/d_0 for the ion-exchange resin and the precursor.

decreases dramatically with increasing CD, and (2) d_α/d_0 for the precursors is less than that for the ion-exchange resins. It is clearly seen that an introduction of crosslinks strongly depresses the swelling power of the resins and precursors.

It is worthy to evaluate the effective crosslinking density, CD_{eff}, which is given from the swelling data with the equation proposed by Errede et al.[14,15] The specific volume, S, of the solvent absorbed by a unit weight of poly(styrene-co-divinylbenzene) at swelling equilibrium is given by,

$$S = C(\lambda^{1/3} - \lambda_0^{1/3}) \qquad (1)$$

where C is the relative swelling power of the absorbed solvent and λ is the average number of carbon atoms in the backbone of the polystyrene segments between crosslink junctions. λ_0 is the value of λ extrapolated to $S = 0$. C and λ_0 were estimated for poly(styrene-co-divinylbenzene) copolymer in toluene solvent: $C = 2.03$ and $\lambda_0 = 1.76$.[14] The effective CDs are calculated with $\lambda = 1/CD_{eff}$. The results are shown in Table I. In low CDs, CD_{eff} is about twice as large as CD (stoichiometric). The discrepancy of the CD and CD_{eff} may results from the difference in the method of copolymer preparation, i.e., living an-

ionic polymerization (Erredo)[14] and suspension polymerization (this work), which leads to the difference in the nature, homogeneous (Erredo) vs. porous and polydisperse (this work). Thus, we use CD not CD_{eff} in this article.

In the case of gel networks immersed in a solvent, the swelling kinetics of the gel swelling triggered by a drastic change of the circumstance, e.g., a change in the solvent quality or temperature, is well described by the Tanaka and Fillmore (TF) theory.[13] The variation of the magnitude of the strain vector, $u(t)$, of a spherical gel immersed in a solvent is given by,

$$u(t) \cong (a_\alpha - a_0) \frac{6}{\pi^2} \sum_{n=1}^{\infty} n^{-2} \exp[-n^2 t/\tau] \qquad (2)$$

where a_α and a_0 are the radius of the gel after and before swelling, respectively, and τ is the characteristic time for swelling. From τ, the cooperative diffusion coefficient of the network, D_c, is given by

$$D_c = a_\alpha^2/\tau \qquad (3)$$

Equation (2) can be approximated to

$$u(t) \sim (a_\alpha - a_0) \frac{6}{\tau^2} \exp[-t/\tau] \qquad (4)$$

except for $0 < t \ll \tau$. Thus an exponential decay is expected in the time variation of the gel strain.

However, the TF theory cannot directly apply to the swelling kinetics of ion-exchange resin because a freeze-dried gel is a porous medium. The TF theory assumes that the diffusant, e.g., water, diffuses from the smooth spherical surface of the gel. On the other hand, a freeze-dried resin has a larger surface area because of its porosity. When the dried resin is immersed, solvent diffuses into the resin much faster than the case of nonporous gel, where the cavities of the porous resin are in-

Table I. Estimation of the Effective CD, CD_{eff}

CD (%)	2	4	8	10	16
d_α/d_0	1.49	1.37	1.16	1.14	1.06
$S = [(d_\alpha/d_0)^3 - 1]$	1.82	1.20	0.40	0.34	0.13
λ	18.8	13.0	7.5	7.2	6.1
CD_{eff} (%)	5	8	13	14	17

S: the specific volume of solvent absorbed by a unit weight of Poly(styrene-co-divinylbenzene) at swelling equilibrium.

λ: the average number of carbon atoms in the "backbone" of the polystyrene segments between cross-link junctions; estimated by eq (1).

stantaneously filled with the solvent by capillary force. Knowing all of these, we assume that (1) the swelling of the assembly (porous resin particles) takes place by two steps [i.e., (i) filling of the cavities with solvent by capillary force and (ii) osmotic diffusion of the solvent into the resin] and (2) the filling time, t_{fill}, is much faster than that of osmotic diffusion, t_{diff}. Therefore, the deterministic process of swelling is the osmotic diffusion. These assumptions allow us to apply the TF theory. Since the solvent filling to the cavities does not result in the size change of the particle, the size change (i.e., swelling) is a consequence of the osmotic diffusion of the solvent to the particles. The time for swelling, t, is corresponding to the diffusion of the solvent molecules to the resin because of $t_{diff} \gg t_{fill}$. Thus, the following equation is given from eq. (4),

$$\ln\left(\frac{d_t - d_\infty}{d_0 - d_\infty}\right) = (\text{const.}) - t/\tau \qquad (5)$$

where d_t denotes the diameter of the particle at time t ($= 0, t$, and ∞). Figure 3 shows the time dependence of the diameter change of the particle. The solid curve in the figure is the results of the curve fitting with eq. (5) and the dashed line corresponds to the TF theory of $n = 5$. The characteristic time, $\tau = 87$ s, is thus obtained in both fittings for CD = 4% and $d_0 = 709$ μm. A similar analysis was conducted for all the samples.

Figure 4(a) shows the plot of τ vs. d_∞^2 for the ion-exchange resins with various CDs. All data points for each CD value roughly fall on a line. Lines in the figure were drawn by a linear regression with a constraint to cross the origin. Here, the characteristic time for swelling, τ, [eq. (3)] has to be reinterpreted because of the porosity of the particle. The rate of solvent diffusion is ruled by the surface area
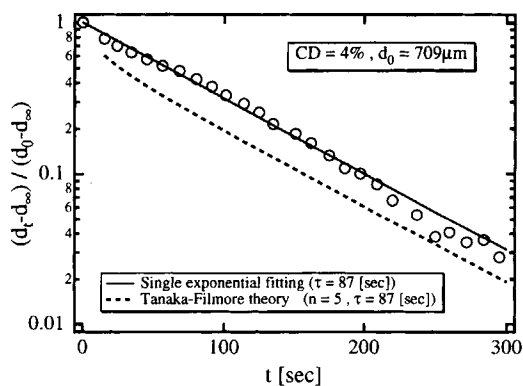

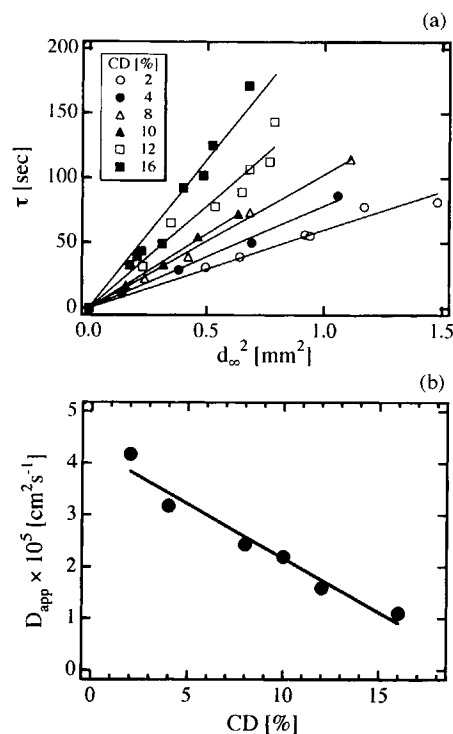**Figure 3** Logarithmic plot of the time dependence of the diameter change for CD = 4% and $d_0 = 709$ μm.

Figure 4 (a) Plot of τ vs. d_∞^2 for the ion-exchange resin having various CDs. Lines were drawn by a linear regression with a constraint to cross the origin. (b) CD dependence of the apparent diffusion coefficient, D_{app}, estimated with eq. (7).

of the particle. If the surface is smooth and dense, eq. (3) applies and the following equaiton is given,

$$\tau = \frac{a_\infty^2}{D_c} = \frac{d_\infty^2}{4D_c} \quad \text{(dense particles)} \qquad (6)$$

However, if the resin is a porous particle, having the surface area, A, τ is expected to be inversely propotional to A. Since the characteristic parameters for the diffusion of the particles are d_∞, A, and D_c, the following equation in a scaling form is given,

$$\tau \sim \frac{1}{A} \frac{d_\infty^\gamma}{D_c} \quad \text{(porous particles)} \qquad (7)$$

where

$$A = f\pi d_\infty^2 \qquad (8)$$

f is the porosity parameter ($f \geq 1$) and γ is the scaling exponent. From the dimensional analysis, γ is obtained to be 4. Thus, from eqs. (7) and (8),

$$\tau \approx \frac{d_\infty^2}{4\pi f D_c} = \frac{d_\infty^2}{4D_{app}} \qquad (9)$$

is obtained, where D_{app} is defined by

$$D_{app} \equiv fD_c. \tag{10}$$

When $f = 1$, eq. (9) becomes identical to eq. (6), i.e., the case of a dense particle. The case of porous particles is corresponding to $f \gg 1$. f is estimated to be in the order of 10 to 10^2 and seems to be a decreasing function of CD because D_c for a typical gel, e.g., polyacrylamide, is about 10^{-7} cm^2/s.

Figure 4(a) shows that D_{app}, i.e., the slope, is dependent on CD. In Figure 4(b) are plotted D_{app} as a function of CD. D_{app} decreases rather linearly with increasing CD. Note that this tendency is completely opposite to the crosslink density dependence of the cooperative diffusion constant of gels. For example, in the case of acrylamide or N-isopropylacrylamide gels, dynamic light scattering observation discloses that the D_c increases linearly with CD, $D_c \sim$ CD.[16] This contradiction may indicate that f is a strong function of CD. The higher the CD, the smaller is f. If f is a scaling function of CD with the exponent, $-\beta$ ($\beta \geq 0$), i.e., $f \sim$ (CD)$^{-\beta}$, D_{app} is given by

$$D_{app} = fD_c \sim (CD)^{-\beta}(CD)^1 = (CD)^{1-\beta} \tag{11}$$

Equation (11) indicates that D_{app} increases with CD for $\beta < 1$ and decreases for $\beta > 1$. Note that the case of $\beta = 0$ is equivalent to the dense particle system. The experimental evidence suggests that the porosity decreases with increasing CD with $\beta > 1$.

The CD dependence of swelling behavior for the precursors was also quite similar to that of ion-exchange resins. The comparison of the swelling kinetics between the precursor and the ion-exchange resin is shown in Figure 5, which demonstrates τ vs. d_∞^2 plots for the precursor in toluene and the ion-exchange resin in water at CD = 4%. Toluene and
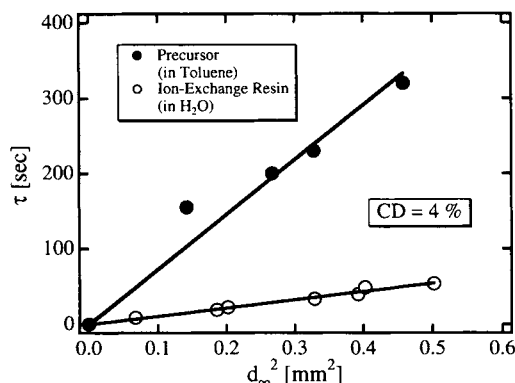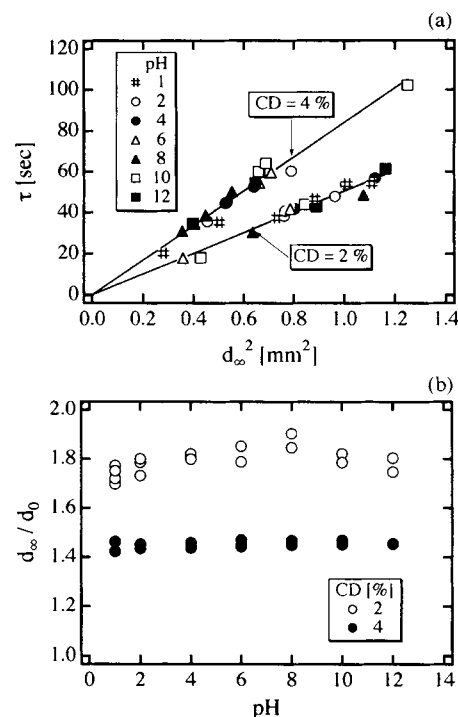
Figure 6 (a) Plot of τ vs. d_∞^2 for the ion-exchange resin at different pHs. (b) pH dependence of the final linear swelling ratio, d_∞/d_0.

water seem to be good solvents for precursor and ion-exchange resin, respectively. From the slopes, we obtain $D_{app} = 4.40 \times 10^{-6}$ [cm^2/s] for the precursor and $D_{app} = 3.18 \times 10^{-5}$ [cm^2/s] for the ion-exchange resin. It was found that D_{app} of ion-exchange resin was about 10 times as large as that of the precursor. It is needless to say that the fast swelling behavior for the ion-exchange resin is due to the electrostatic repulsive interactions and the Donnan potential created in the resins by immersion. The estimated D_{app}s are much larger than D_c of typical gels, such as polyacrylamide gel, for which D_c is in the order of 10^{-7} [cm^2/s].[17] This is due to the porosity of the resin as discussed above.

Let us discuss the effect of the surrounding solution on the swelling behavior. Figure 6(a) shows τ vs. d_∞^2 plots for ion-exchange resin at different pHs. According to eq. (9) and the assumptions (1) and (2), the data points are expected to align on a straight line crossing the origin and the slope gives the inverse of the diffusion constant. As shown in the figure, data points with the same CD are on a line regardless of pH, which indicates that τ (or D_{app}) is independent of pH on the swelling behavior. Figure 6(b) also proves that the final linear swelling ratio, d_∞/d_0, is independent of pH. The invariance of τ and d_∞/d_0 with pH results from the strong dissociation

Figure 5 Plot of τ vs. d_∞^2 for the ion-exchange resin in water and the precursor in toluene at CD = 4%.

power of sulfonic acid group, i.e., $pK_d < 1$,[1-3] where K_d is the dissociation constant of sulfonic groups. Therefore, all the sulfonic groups are dissociated in a solution even at pH 1.

Figure 7 shows d_∞/d_0 vs. log C_{salt}, plots for ion-exchange resins of CD = 2%, 4%, and 8%. As shown in the figure, d_∞/d_0 is a strong decreasing function with C_{salt} for the case of CD = 2%. However, the higher the CD, the less the d_∞/d_0 changes with log C_{salt}. For CD ≥ 8%, C_{salt} dependence of d_∞/d_0 was hardly observed. Changes of the log C_{salt} dependence of d_∞/d_0 are seen at the concentrations indicated with arrows. Above these concentrations, the electrostatic interactions between charges on the resin seems to be highly screened and the equilibrium swelling becomes similar to a noncharged resin, i.e., the precursors. It was inferred from Figures 6 and 7 that CD is one of the most important parameters determining the swelling behavior.

SANS

Figure 8 shows the double logarithmic plots of SANS intensity functions of ion-exchange resin and precursor having several CDs. Two important features should be noted here. (1) No noticeable CD dependence is found both in the ion-exchange resins or the precursors except for the case of CD = 2%. (2) The absolute scattered intensities are in the same order even the system is quite different, i.e., ion-exchange resins in deuterated water vs. crosslinked polystyrene precursors in deuterated toluene.

The former indicates that the microstructure is quite similar regardless of CD at least in this spatial-length window, i.e., from a few tens to a few hundreds of angstroms. The profiles in the figure can be well described with a power law function,
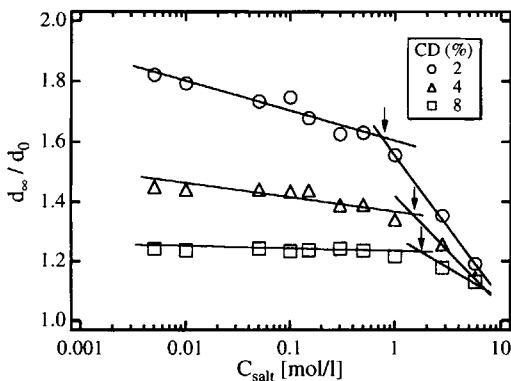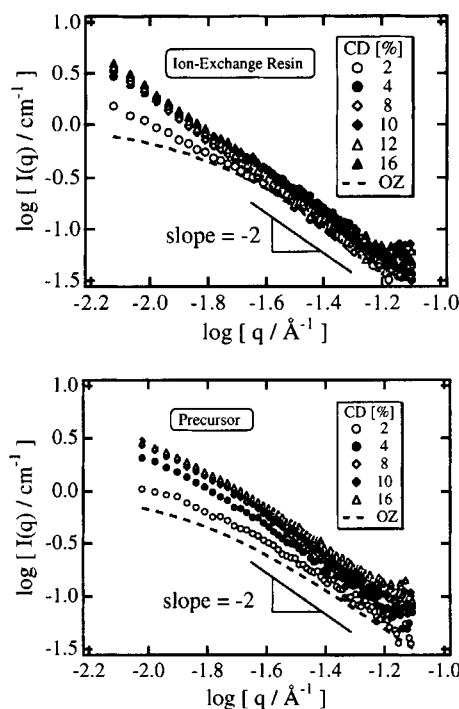

Figure 8   Double logarithmic plot of SANS intensity functions of ion-exchange resin and the precursor having several CDs. Dashed curves show Ornstein–Zernike functions of $\xi = 70$ Å.

$$I(q) \sim q^{-D} \tag{12}$$

where q and D are the magnitude of the scattering vector and the mass-fractal dimension, respectively.[19] Therefore, the slope of the profiles in the figure is equal to D. D was estimated to be ~ 2, indicating that the resin consisted of a rather coarsely interconnected domains irrespective of CD in the swelling equilibrium. A microscopic model for the resin as well as the precursors will be given in the next section.

For comparison, the results of the fitting with the Ornstein–Zernike (OZ) function given by

$$I(q) \sim (1 + \xi^2 q^2)^{-1} \tag{13}$$

Figure 7   Salt concentration, C_{salt}, dependence of d_∞/d_0 for the ion-exchange resin.

is also shown with the dashed curves, where ξ is the correlation length. ξ is chosen here to be 70 Å. $I(q)$s for the precursor and ion-exchange resin of CD = 2% seem to be well described by eq. (13). Though the OZ function also scales as q^{-2} at large q, the deviation from the experimental results at low q region is obvious, particularly for the case of the ion-exchange resin. Thus, we believe that the power law function is more suitable to describe the systems.

The second feature indicates that ion-exchange resin and the precursor have the almost same SANS intensity at all CDs. Now we compare the contrast factor of SANS in the two cases. The contrast factor of neutron scattering, K_{ij}, are given by

$$K_{ij} = N_A v_j \left(\frac{\alpha_i}{v_i} - \frac{\alpha_j}{v_j} \right)^2 \qquad (14)$$

where N_A denotes Avogadro's number. α_k and v_k are the scattering length and the molar volume of the k ($= i$ or j) component, respectively. Table II shows K_{ij} for ion-exchange resin/deuterated water and the precursor/deuterated toluene. The molar volumes were estimated by measuring the mass densities of the resin and the precursors by gravimetry. Note that the 40% sulfonation and ionization of the sulfonic group, i.e., SO_3^-, are taken into account for the calculation of K_{ij} for the ion-exchange resin. It is rather surprising to realize that two contrast factors are almost the same. By knowing that the similarity of the scattering contrasts between the two systems, it is now reasonable to expect that the SANS intensity functions from the two systems are in the same order.

The two features disclosed above directly lead to the following conclusion. The microstructure of styrene precursors is little changed by introducing sulfonate groups.

Proposed Structure Model

Based on the results shown above, we now propose a possible structure model for ion-exchange resin which satisfies the experimental findings. Figure 9 shows the schematic representation of a macroscopic network model which accounts for the swelling behavior of the resin. The circles, lattice, and dots indicate the size of ion-exchange resin, polystyrene networks, and crosslinking points, respectively. Suppose that the size of ion-exchange resin with high CD at swelling equilibrium is the same as that
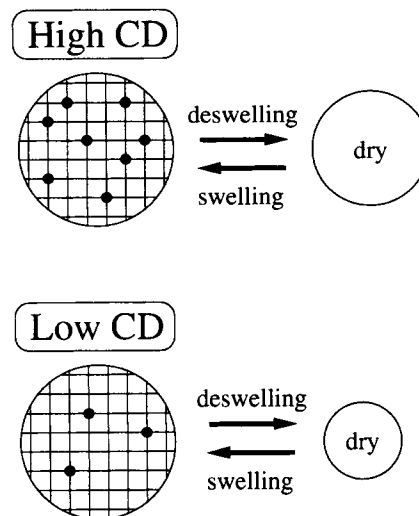
Table II.   SANS Contrast Factors of D_2O/Ion-Exchange Resin and Deuterated Toluene (D-Toluene)/Precursor

i/j	K_{ij} (cm^{-1})
D_2O/ion-exchange resin	0.341
D-toluene/precursor	0.302

Mass densities are evaluated by gravimetry: ion-exchange resin; 1.31 g/cm^3, precursor; 1.05 g/cm^3.

Figure 9   Schematic representation of the network models having high and low crosslinking densities.

with low CD. If so, the polymer concentrations are the same in both resins. In this case, the difference in CD may not affect the microstructure of resin, which was proved in the SANS experiments. However, on a shrinking process, the resin with high CD should shrink less than that with low CD because of topological constraints. The inverse is obvious, i.e., the dried resin having high CD will swell less than the resin having low CD, which agrees with the results of swelling experiment described above.

The supposition that the size of ion-exchange resin having high CD at swelling equilibrium was the same as that having low CD was proved by evaluating the size distribution of the resin particles at both dried and swollen states. A diameter distribution measurement was made on 100 particles which were arbitrarily chosen. Figure 10 shows the histogram of distributions of the particle diameter at CD = 2% and 8%, where n is the population of particles and the open and hatched columns are corresponding to the number of dried and swollen particles, respectively. At CD = 2%, the medians in swollen and dried states are 0.78 and 0.4 mm, respectively, the ratio of which [1.97 (= 0.78/0.4)] is in good accordance with d_α/d_0 in Figure 2. On the other hand, the corresponding ratio of medians for CD = 8% is 1.23 (= 0.81/0.66), which is much smaller than that for CD = 2%. Figure 10 clearly indicates that the medians at the swollen state (hatched columns) are almost the same both at CD = 2% and 8%. This supports our supposition, i.e., an equivalency of the size and structure at the swollen state irrespective of CD.

Now we discuss a microscopic model of the resin. Figure 11 shows the schematic models of the network structure for (a) ion-exchange resin and (b) typical polymer gels. In the case of ion-exchange resin, the precursors are prepared by suspension polymerization. The polymerization takes place in "oil droplets" of monomers and crosslinkers dispersed in water. Crosslinking reaction is initiated from seeds (initiator molecules) followed by successive polymerization and crosslinking. Since the monomer reaction ratio of divinylbenzene (crosslinkers) is larger than styrene (monomers), the crosslinking degree has a gradient with polymerization time, i.e., higher at the beginning and lower at the end. This leads to a highly heterogeneous microstructures in a droplet as shown in Figure 11(a), which has a self-similar nature. Thus, the corresponding scattering function has a power law behavior. On the other hand, polymer gels are usually prepared in a homogeneous medium, for example, polyacrylamide in water. This results in a rather uniform network formation as illustrated in Figure 11(b). The scattering function from such a gel has a power law behavior at high q ($> \xi$) where ξ is a mesh size of the network.[19] However, for $q < \xi$, the scattering function has a tendency to level off as q approaches zero. Furthermore, there is a strong CD dependence in the scattering function for typical gels as reported by Cohen et al.[20] This kind of CD dependence was not observed in the ion-exchange resins studied here. This also indicates
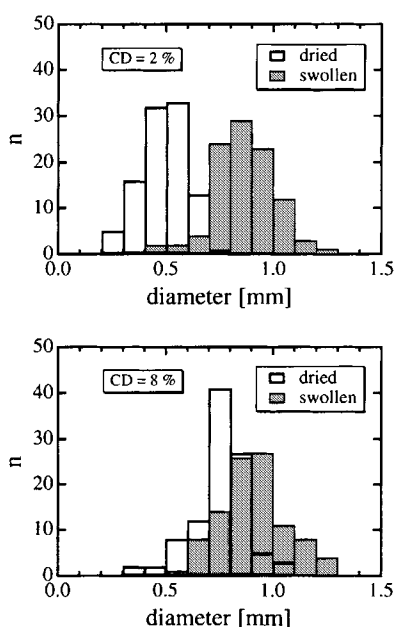

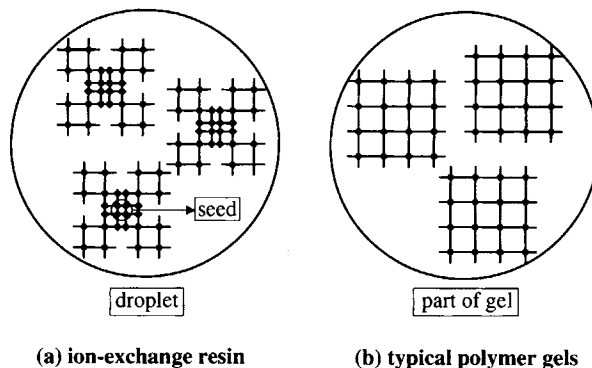(a) ion-exchange resin   (b) typical polymer gels

Figure 11 Schematic models of the network structure for (a) ion-exchange resin and (b) typical polymer gels.

that the ion-exchange resin has a fractal nature due to the heterogeneous polymerization.

CONCLUDING REMARKS

The swelling behavior and microstructure of ion-exchange resin were investigated by swelling measurements and SANS. It was found from the swelling experiment that the swelling kinetics of ion-exchange resin in water was not affected by pH or C_{salt} but on the CD. The swelling kinetics was simply described by a single-exponential function, which applies to the cooperative diffusion of polymer gels. However, the effective diffusion constant is not D_c but $D_{app} = f D_c$, where f is the parameter indicating the porosity of the particles. f is in the order of 10 to 10^2 and seems to be a decreasing function of CD. This is why D_{app} is much lareger than that of typical gels. The rate-deterministic process of the swelling is the osmotic diffusion of the solvent. SANS profiles proved that the microstructure of ion-exchange resins having different CDs at liquid saturation was surprisingly constant, and the resin consisted of a rather coarsely interconnected domains irrespective of CD. These results are consistent with a model in which the ion-exchange resins had the same diameters owing to copolymerization at the swelling equilibrium state and the effect of crosslinking is manifested during subsequent evaporation to droplet, i.e., the shrinking process. The magnitude of this shrinkage varies inversely with CD.

Figure 10 Histograms of distributions of the particle diameter for ion-exchange resin at CD = 2% and 8%.

REFERENCES AND NOTES

1. R. L. Albright and P. A. Yarnell, in *Encyclopedia of Polymer Science and Engineering*, 2nd ed., Vol., 8, John Wiley & Sons, Inc., New York, 1985, p. 341.
2. K. Dorfner (Ed.), *Ion Exchangers*, Walter de Gruyter, Berlin, 1991.
3. *DIAION* (Japanese), Mitsubishi Chemical Co., 1992.
4. F. Schosseler, F. Ilmain, and S. J. Candau, *Macromolecules*, **24**, 225 (1991).
5. F. Schosseler, A. Moussaid, J. P. Munch, and S. J. Candau, *J. Phys. II (Paris)*, **1**, 1197 (1991).
6. M. Shibayama, T. Tanaka, and C. C. Han, *J. Chem. Phys.*, **97**, 6842 (1992).
7. A. M. Fernandez, J. M. Widmaier, L. H. Sperling, and G. D. Wignall, *Polymer*, **25**, 1718 (1984).
8. J. G. Weissman and L. H. Sperling, *Macromolecules*, **18**, 1720 (1985).
9. M. Wojaczynska and B. N. Kolarz, *J. Appl. Polym. Sci.*, **56**, 433 (1995).
10. P. P. Wieczorek, M. Iravsky, B. N. Kolarz, and K. Dusek, *J. Appl. Polym. Sci.*, **27**, 277 (1982).
11. D. Schwahn, H. Takeno, L. Willner, H. Hasegawa, H. Jinnai, T. Hashimoto, and M. Imai, *Phys. Rev. Lett.*, **73**, 3427 (1994).
12. D. Schwahn, S. Janssen, and T. Springer, *J. Chem. Phys.* **97**, 8775 (1992).
13. T. Tanaka and D. J. Fillmore, *J. Chem. Phys.*, **70**, 1214 (1979).
14. L. A. Errede, *Macromolecules*, **19**, 654 (1986).
15. L. A. Errede and S. C. Hanson, *J. Appl. Polym. Sci.*, **54**, 619 (1994).
16. M. Shibayama, T. Norisuye, and S. Nomura, to appear.
17. T. Tanaka, L. O. Hocker, and G. B. Benedek, *J. Chem. Phys.*, **59**, 5151 (1973).
18. J. E. Martin and B. J. Ackerson, *Phys. Rev.*, **A31**, 1180 (1985).
19. A. Baumgartner and C. E. Picot (Eds.), *Molecular Basis of Polymer Networks*, Springer–Verlag, Berlin, 1989.
20. Y. Cohen, O. Ramon, I. J. Kipelman, and S. Mizrahi, *J. Polym. Sci., Polym. Phys. Ed.*, **30**, 1055 (1992).